JOC Articles

Investigation of the Mechanism of the Intramolecular Scholl Reaction of Contiguous Phenylbenzenes

Pawel Rempala, Jiří Kroulík, and Benjamin T. King*

University of Nevada, Reno, Department of Chemistry, Reno, Nevada 89557

king@chem.unr.edu

Received December 30, 2005

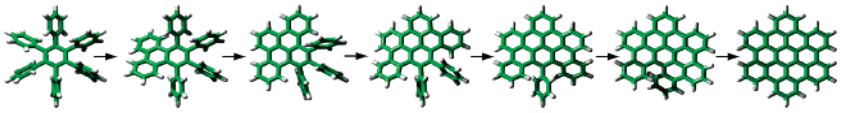

Two mechanisms of the Scholl reaction were investigated in the series 1, 2, ..., *n*-oligophenylbenzenes ($n = 2, 3, 4, 6$) at the B3LYP/6-31G(d) level of theory. A mechanism involving generation of a radical cation followed by C−C bond formation and dehydrogenation is unlikely on the basis of unfavorable energies of activation. A mechanism involving generation of an arenium cation followed by C−C bond formation and dehydrogenation is energetically feasible. An explanation for the facile polycondensation of hexaphenylbenzene to hexa-*peri*-hexabenzocoronene, where six new aryl−aryl bonds are formed, is provided. Kinetic simulations based on the calculated activation energies of the arenium cation mechanism predict that intermediates will not accumulate; this is supported by mass balance experiments. Reaction optimization studies suggest that $PhI(O_2CCF_3)_2/BF_3{\cdot}OEt_2$ or $MoCl_5$ are superior to $FeCl_3$ or $AlCl_3/CuCl_2$. This is a full account of our work reported partially as a communication previously (Rempala, P.; Kroulík, J.; King, B. T. *J. Am. Chem. Soc.* **2004**, *126*, 15002−15003).

Introduction

Dehydrogenative aryl−aryl bond formation can be accomplished in many ways. Treatment with a Lewis acid (**1** → **2**),[2,3] base (**3** → **4a** + **4b**),[4] or oxidant (**5** → 6),[5] irradiation in the presence of oxidant (**7** → 8),[6] melting under vacuum (**9** → **10**),[7] and heterogeneous catalysis at high temperature (**11** → **12**)[8−10] were used successfully (Scheme 1). These reactions are attractive because functionality is usually not required.

The Scholl reaction, understood as the condensation of aromatics under the influence of a Lewis acid,[11] often $AlCl_3$, works well for dendritic oligo- and polyphenylene compounds. Müllen and co-workers have used this reaction to convert dendritic oligophenylenes to the corresponding symmetric hydrocarbons forming as many as 126 new C−C bonds in a single step.[12−15] In contrast to such reactions, the simple cyclization of *o*-terphenyl, which requires forming just one C−C bond, was not successful in our hands using a variety of Scholl conditions.[16]

Hexa-*peri*-hexabenzocoronene (HBC, **10**) is synthesized in excellent yields from hexaphenylbenzene (C_6Ph_6, **13**, Scheme 2a).[17,18] Müllen and co-workers have shown that this reaction

(1) Rempala, P.; Kroulík, J.; King, B. T. *J. Am. Chem. Soc.* **2004**, *126*, 15002−15003.
(2) Scholl, R.; Mansfeld, J. *Ber. Dtsch. Chem. Ges.* **1910**, *43*, 1734−1746.
(3) Balaban, A. T.; Nenitzescu, C. D. Dehydrogenation Condensation of Aromatics (Scholl and Related Reactions). In *Friedel−Crafts and Related Reactions*; Olah, G., Ed.; Wiley: New York, 1964; Vol. 2, pp 979−1047.
(4) Bradley, W.; Sutcliffe, F. K. *J. Chem. Soc.* **1952**, 1247−1251.
(5) Pummerer, R.; Prell, E.; Rieche, A. *Ber. Dtsch. Chem. Ges.* **1926**, *59*, 2159−2161.
(6) Mallory, F. B.; Wood, C. S.; Gordon, J. T.; Lindquist, L. C.; Savitz, M. L. *J. Am. Chem. Soc.* **1962**, *84*, 4361−4362.
(7) Clar, E.; Ironside, C. T.; Zander, M. *J. Chem. Soc.* **1959**, 142−148.
(8) Scola, D. A. *J. Chem. Eng. Data* **1964**, *9*, 405.
(9) Copeland, P. G.; Dean, R. E.; McNeil, D. *J. Chem. Soc.* **1960**, 1687−1689.
(10) Hansch, C.; Geiger, C. F. *J. Org. Chem.* **1958**, *23*, 477−478.
(11) Li, J. J. *Name Reactions: A Collection of Detailed Reaction Mechanisms*, 2nd ed.; Springer-Verlag: New York, 2003.
(12) Simpson, C. D.; Brand, J. D.; Berresheim, A. J.; Przybilla, L.; Räder, H. J.; Müllen, K. *Chem. Eur. J.* **2002**, *8*, 1424−1429.
(13) Iyer, V. S.; Wehmeier, M.; Brand, J. D.; Keegstra, M. A.; Müllen, K. *Angew. Chem., Int. Ed. Engl.* **1997**, *36*, 1604−1607.
(14) Watson, M. D.; Fechtenkötter, A.; Müllen, K. *Chem. Rev.* **2001**, *101*, 1267−1300.
(15) Simpson, C. D.; Mattersteig, G.; Martin, K.; Gherghel, L.; Bauer, R. E.; Räder, H. J.; Müllen, K. *J. Am. Chem. Soc.* **2004**, *126*, 3139−3147.
(16) Kroulík, J.; Robertson, C. R.; Hilton, C. L.; Korinek, J. D.; Gortari, L. M.; Rempala, P.; King, B. T. Manuscript in preparation.
(17) Ito, S.; Wehmeier, M.; Brand, J. D.; Kübel, C.; Epsch, R.; Rabe, J. P.; Müllen, K. *Chem. Eur. J.* **2000**, *6*, 4327−4342.
(18) Kübel, C.; Eckhardt, K.; Enkelmann, V.; Wegner, G.; Müllen, K. *J. Mater. Chem.* **2000**, *10*, 879−886.

10.1021/jo0526744 CCC: $33.50
Published on Web 06/16/2006

SCHEME 1. Examples of Dehydrogenation Coupling Reactions of Aromatic Compounds[a]

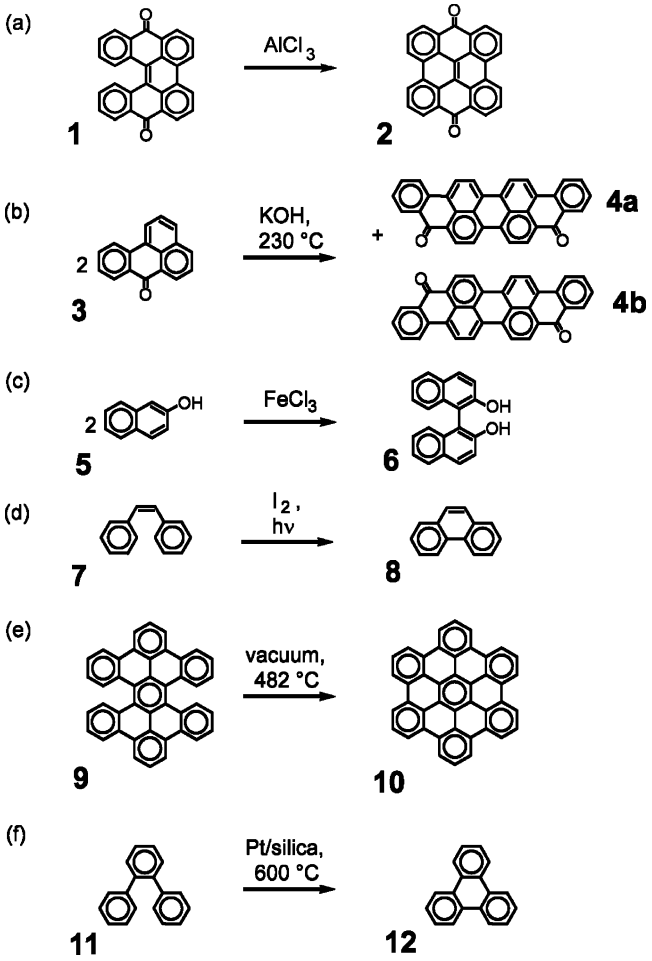

[a] Key: (a) ref 2, (b) ref 4, (c) ref 5, (d) ref 6, (e) ref 7, (f) refs 8−10.

is intramolecular. In one case, an intermediate lacking two C−C bonds (**14**) was obtained in low yield when insufficient oxidant was used (Scheme 2a).[18] Intermediates with two and four new CC bonds were also reported as present in the reaction mixture based on FD-MS but were not isolated. An early report[19] on the preparation of HBC from C_6Ph_6 under Scholl conditions ($NaCl/AlCl_3$ melt, air) appeared in the patent literature and claimed that three incompletely cyclized structures (**15**, **16**, **17**) could be obtained along with HBC (Scheme 3b). While HBC was unequivocally characterized, the partially cyclized intermediates were not. These putative intermediates can be attributed to low solubility of the reactants and intermediates in the polar $AlCl_3/NaCl$ melt.

We aim to explain the ease of polycondensation, elusiveness of intermediates, and lack of generality of the Scholl reaction by examining its mechanism using computational and experimental chemistry. Aside from our own communication,[1] there is apparently only one computational study of the Scholl reaction.[20]

In the Scholl reaction,[3] oxidative aryl−aryl coupling reactions are commonly effected by a transition metal halide, which can act both as a Lewis acid and an oxidant, as developed by Kovacic and co-workers.[21−23] A mechanism similar to the arenium cation mechanism was proposed as early as 1935[24] and refined by Nenitzescu and Balaban.[25] In their review,[3] the arenium cation and radical cation[3,26] mechanisms were juxtaposed (Scheme 4).

In the arenium cation mechanism, an aromatic compound (**18**) is protonated, and the resulting electrophilic σ complex (**19**) reacts with another aromatic core to generate a new C−C bond. Deprotonation gives intermediate **20**, and dehydrogenation restores aromaticity to afford the condensed product, **21**. The isolation of a dihydro analogue of **20** has been reported.[27]

Brønsted acids are implicated as catalysts in the Scholl reaction. Traces of HCl or water accelerate the reaction,[3,24] presumably by reaction with $AlCl_3$ to generate $H[AlCl_3OH]$ and HCl. Indeed, the reaction proceeds in anhydrous HF,[28,3] which is not an oxidizing acid. Of course, any acid, Lewis or Brønsted, could form the key arenium intermediate. Our calculations focused on Brønsted acids because they are likely to be present in the reaction mixture and because they are computationally tractable.

In the second proposed mechanism, a radical cation, **22**, is first generated by one-electron oxidation of the starting material. Its subsequent electrophilic C−C bond-forming reaction with another aromatic group, deprotonation, and formal loss of H atom from intermediate **23**, follow.

The generation of aryl radical cations under oxidizing conditions is precedented. When treated with Lewis acids or with concentrated sulfuric acid, many PAHs give paramagnetic solutions,[3] and therefore, radical cations may be present in the Scholl reaction. This, however, does not necessarily mean they are productive reactive intermediates. Phenols do probably

SCHEME 2. Two[18,19] HBC Syntheses

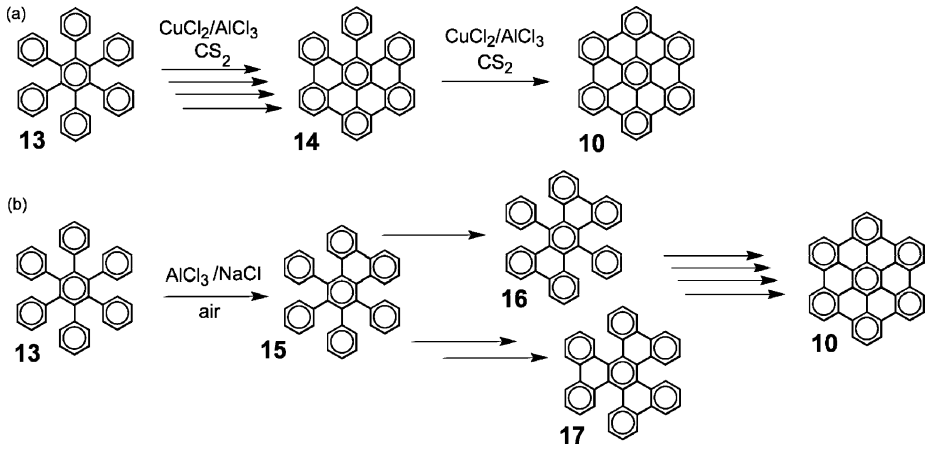

SCHEME 3. Proposed Mechanisms of the Scholl Reaction: (a) Arenium Cation Mechanism; (b) Radical Cation Mechanism

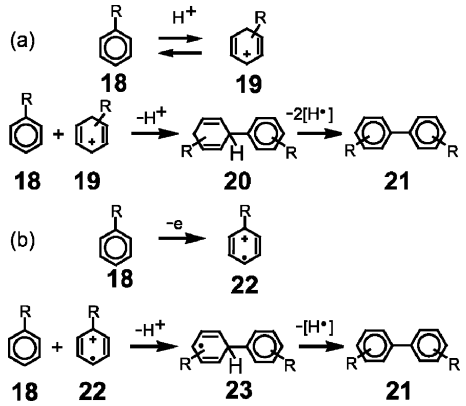

SCHEME 4. Scholl Condensation on Heterocycles

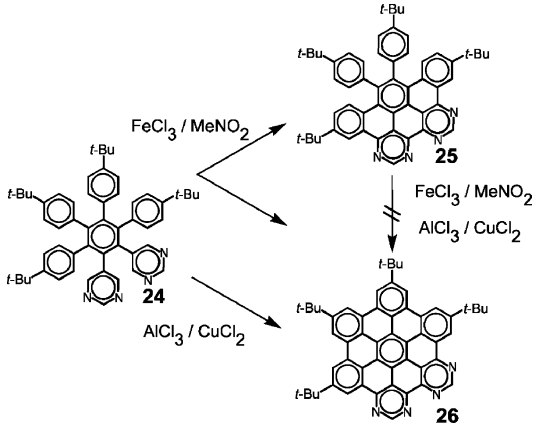

undergo coupling via a radial mechanism. The mechanism proposed by Pummerer, dimerization of phenoxy radical, followed by tautomerization,[29] is widely accepted. This mechanism is, however, unlikely in substrates that do not form long-lived radicals. For both mechanisms (Scheme 3a,b), generalization to intramolecular case, where R is linker, is easily envisioned.

Di Stefano et al.[20] recently investigated the intramolecular condensation of *o*-terphenyl or C_6Ph_6, coupled with reduction of $CuCl_2$, at the B3LYP/3-21G level of theory. The investigation, which focused on a radical cation mechanism, was based on two postulates: oxidants are required but Brønsted acids are not required. We prefer a less restrictive set of postulates: an acid, Lewis or Brønsted, is required and the reaction is formally an oxidation.

Many of their results agree well with our work on radical cation mechanism. Specifically, the C−C bond formation of radical cations is endothermic by ∼22 kcal/mol, its reverse reaction is characterized by a very low energy barrier (2 kcal/mol), the gas-phase formation of radical cations using $CuCl_2$ is strongly endergonic, and bonds are contiguously formed.[20]

Cases involving heterocycles, like the condensation of 1,2-dipyrimidyl-3,4,5,6-tetra(4-*tert*-butylphenyl)benzene (**24**),[30] require special consideration (Scheme 4). We propose that an arenium mechanism also applies. A protonated or doubly protonated pyrimidine ring could act as an electrophile, explaining bond formation to the pyrimidine rings. The *N*-protonated PAH core might be insufficiently electrophilic to attack the adjacent phenyl ring. Protonation of the phenyl rings will be difficult since the basic nitrogen sites will be protonated and bear a positive charge. Even if protonation of the phenyl substitutents was possible, the *N*-protonated PAH core would be a poor nucleophile, inhibiting electrophilic attack. The chelating substrate complicates the mechanistic analysis. Different reactants, $FeCl_3$ or $AlCl_3/CuCl_2$, give different product distributions, presumably because the metals coordinate differently. It is notable that **25** is not converted to **26** by treatment with $AlCl_3/CuCl_2$, indicating that **25** is not an intermediate in the $AlCl_3/CuCl_2$ induced conversion of **24** to **26**.

Computational Details

Density functional calculations were performed using Gaussian 03[31] and Gaussian 98[32] programs. The B3LYP functional[33−35] together with standard 6-31G(d) basis set[36] (Cartesian *d* functions) was used. DFT calculations on radical ions are problematic;[37]

(19) Halleux, A. L. US 3,000,984, 1961.
(20) Di Stefano, M.; Negri, F.; Carbone, P.; Müllen, K. *Chem. Phys.* **2005**, *314*, 85−99.
(21) Kovacic, P.; Koch, F. W. *J. Org. Chem.* **1965**, *30*, 3176−3181.
(22) Kovacic, P.; Jones, M. B. *Chem. Rev.* **1987**, *87*, 357−379.
(23) Kovacic, P. Reactions of Aromatics with Lewis Acid Metal Halides. In *Friedel−Crafts and Related Reactions*; Olah, G., Ed.; Wiley: New York, 1965; Vol. 4, pp 111−126.
(24) (a) Baddeley, G. *J. Chem. Soc.* **1950**, 994−997. (b) Baddeley, G.; Kenner, J. *J. Chem. Soc.* **1935**, 303−309.
(25) Balaban, A. T.; Nenitzescu, C. D. *Acad. Repub. Pop. Rom., Fil. Cluj. Stud. Cercet. Chim.* **1959**, *7*, 521−529. Nenitzescu, C. D.; Balaban, A. T. *Chem. Ber.* **1958**, *91*, 2109−2116.
(26) Rooney, J. J.; Pink, R. C. *Trans. Faraday Soc.* **1962**, *58*, 1632−1641.
(27) Clar, E. *Ber. Dtsch. Chem. Ges.* **1930**, *63*, 112−120.
(28) Simons, J. H.; McArthur, R. E. *J. Ind. Eng. Chem.* **1947**, *39*, 364−367.
(29) Pummerer, R.; Luther, F. *Ber. Dtsch. Chem. Ges.* **1928**, *61*, 1102−1107.
(30) Gregg, D. J.; Bothe, E.; Höfer, P.; Passaniti, P.; Draper, S. M. *Inorg. Chem.* **2005**, *44*, 5654−5660.
(31) Frisch, M. J.; Trucks, G. W.; Schlegel, H. B.; Scuseria, G. E.; Robb, M. A.; Cheeseman, J. R.; Montgomery, J. A., Jr.; Vreven, T.; Kudin, K. N.; Burant, J. C.; Millam, J. M.; Iyengar, S. S.; Tomasi, J.; Barone, V.; Mennucci, B.; Cossi, M.; Scalmani, G.; Rega, N.; Petersson, G. A.; Nakatsuji, H.; Hada, M.; Ehara, M.; Toyota, K.; Fukuda, R.; Hasegawa, J.; Ishida, M.; Nakajima, T.; Honda, Y.; Kitao, O.; Nakai, H.; Klene, M.; Li, X.; Knox, J. E.; Hratchian, H. P.; Cross, J. B.; Adamo, C.; Jaramillo, J.; Gomperts, R.; Stratmann, R. E.; Yazyev, O.; Austin, A. J.; Cammi, R.; Pomelli, C.; Ochterski, J. W.; Ayala, P. Y.; Morokuma, K.; Voth, G. A.; Salvador, P.; Dannenberg, J. J.; Zakrzewski, V. G.; Dapprich, S.; Daniels, A. D.; Strain, M. C.; Farkas, O.; Malick, D. K.; Rabuck, A. D.; Raghavachari, K.; Foresman, J. B.; Ortiz, J. V.; Cui, Q.; Baboul, A. G.; Clifford, S.; Cioslowski, J.; Stefanov, B. B.; Liu, G.; Liashenko, A.; Piskorz, P.; Komaromi, I.; Martin, R. L.; Fox, D. J.; Keith, T.; Al-Laham, M. A.; Peng, C. Y.; Nanayakkara, A.; Challacombe, M.; Gill, P. M. W.; Johnson, B.; Chen, W.; Wong, M. W.; Gonzalez, C.; Pople, J. A. *Gaussian 03*; Revision B.02. Gaussian, Inc.: Pittsburgh, PA, 2003.
(32) Frisch, M. J.; Trucks, G. W.; Schlegel, H. B.; Scuseria, G. E.; Robb, M. A.; Cheeseman, J. R.; Zakrzewski, V. G.; Montgomery, J. A., Jr.; Stratmann, R. E.; Burant, J. C.; Dapprich, S.; Millam, J. M.; Daniels, A. D.; Kudin, K. N.; Strain, M. C.; Farkas, O.; Tomasi, J.; Barone, V.; Cossi, M.; Cammi, R.; Mennucci, B.; Pomelli, C.; Adamo, C.; S. Clifford, S.; Ochterski, J.; Petersson, G. A.; Ayala, P. Y.; Cui, Q.; Morokuma, K.; Rega, N.; Salvador, P.; Dannenberg, J. J.; Malick, D. K.; Rabuck, A. D.; Raghavachari, K.; Foresman, J. B.; Cioslowski, J.; Ortiz, J. V.; Baboul, A. B.; Stefanov, B. B.; Liu, G.; Liashenko, A.; Piskorz, P.; Komaromi, I.; Gomperts, R.; Martin, R. L.; Fox, D. J.; Keith, T.; Al-Laham, M. A.; Peng, C. Y.; Nanayakkara, A.; Challacombe, M.; Gill, P. M. W.; Johnson, B.; Chen, W.; Wong, M. W.; Andres, J. L.; Gonzalez, C.; Head-Gordon, M.; Replogle, E. S.; Pople, J. A. *Gaussian 98*; Revision A.11.4. Gaussian, Inc.: Pittsburgh, PA, 2002.
(33) Becke, A. D. *J. Chem. Phys.* **1993**, *98*, 5648−5652.
(34) Becke, A. D. *Phys. Rev. A* **1988**, *38*, 3098−3100.
(35) Lee, C.; Yang, W.; Parr, R. G. *Phys. Rev. B* **1988**, *37*, 785−789.
(36) Hariharan, P. C.; Pople, J. A. *Theor. Chim. Acta* **1973**, *28*, 213−222.

therefore, the BHandHLYP functional was also tested in the case of *o*-terphenyl, as it is capable of locating transition states on radical ion potential surfaces that are difficult to find with the B3LYP functional.[38] Standard cutoff values were used in geometry optimizations. Stationary points were subjected to frequency calculations and assigned as minima (all real frequencies) or transition states (exactly one imaginary frequency); this also provided G_{298}. For doublet species (radical ions), the expectation values of S^2 were within 0.03 of the exact value, 0.75. Use of molecular symmetry was deliberately avoided in radical cations. Wave function stability calculations were performed for *o*-terphenyl doublet species. Single-point solvation calculations (evaluating ΔG_{solv}, with SCFVAC option) were performed with polarizable continuum model,[39,40] as implemented in Gaussian 03, with a dielectric constant of 8.93 (CH_2Cl_2). Atomic radii optimized for the HF level of theory were applied (radii = UAHF). No scaling factor was used for frequencies in the evaluations of thermodynamic functions, and no attempt was made to treat any low-frequency vibrations as internal rotations.

Results and Discussion

***o*-Terphenyl Coupling: Arenium Cation Mechanism.** In the arenium cation mechanism for the intramolecular C−C bond-forming reaction of *o*-terphenyl, protonation of a peripheral phenyl ring at sites leading to favorable charge density ortho (position 3) and para (position 5) with respect to the new C−C bond was considered. Although these are not the most basic site in *o*-terphenyl, the differences in calculated proton affinities between various sites are small. Since these protonated *o*-terphenyl tautomers, which are also rotamers, are in rapid equilibrium, the Curtin−Hammet principle applies:[41] the reaction pathway is defined by lowest absolute energy transition states, not the relative population of tautomers or by their relative activation energies. Both trans and cis geometries of the electrophilic intermediates and transition states were considered. The full mechanism of triphenylene formation via the ortho protonation, trans pathway is shown in Scheme 5.

To identify the rate-limiting step, proton transfer and dehydrogenation transition states must also be considered. Because the exact nature of these elementary reactions is unclear, calculations of these transition states were not attempted. Rather, activation parameters for related processes were taken from the literature. Proton transfer in a model hydronium ion−benzene system was calculated recently[42] to have a barrier in vacuo of 4 kcal/mol; proper treatment of the problem required sophisticated calculations, which are currently not feasible for larger systems. Instead, this value was taken as the energy of proton-transfer transition states ($\Delta G^{\ddagger}$ and $\Delta H^{\ddagger}$) relative to higher energy of the two species that this transition state connects. The experimental value for the rate constant of the pseudo-first-order loss of deuterium from C_6H_5D in 83 wt % H_2SO_4 is 3.45×10^{-4} s^{-1} at 25 °C,[43] which corresponds to a half-life of 33 min, indicating process somewhat less feasible than that characterized by 4 kcal/mol activation barrier. However, the measured rate was strongly dependent on the acidity function.

SCHEME 5. Arenium Cation Pathways for the Condensation of *o*-Terphenyl with Ortho or Para Protonations and Cis or Trans C−C Bond Formation

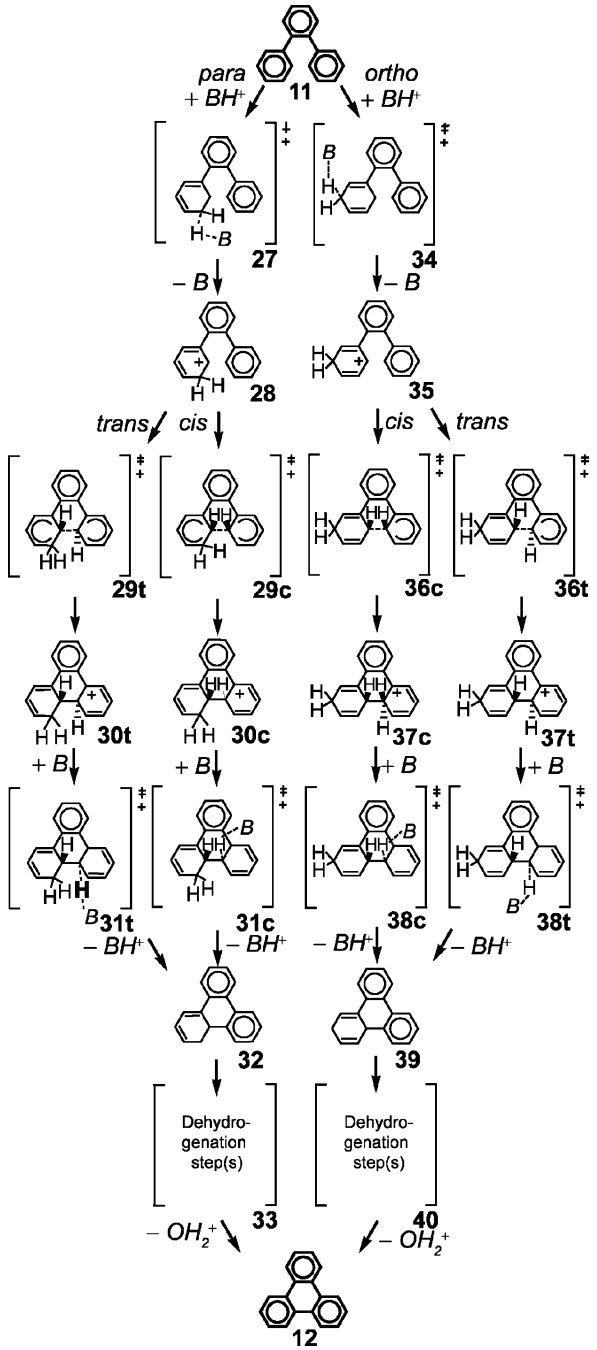

In our mechanism, the presence of superacid is postulated, and we adopt therefore the value from ab initio calculations.

The strength of the catalytic acid is an important thermodynamic parameter. The relative energies of the starting material (*o*-terphenyl) and the final product (triphenylene + oxidation product of hydrogen, or H_2 itself) do not depend on acid strength, since the acid is a catalyst. The same holds for all neutral intermediates considered (see below). The effect of acid strength on the reaction coordinate diagram is straightforward. The use of weaker acids results in more endergonic initial protonation; the use of stronger acids results in more exergonic initial protonation. We chose an acid that gives a thermoneutral initial protonation: protonated *o*-terphenyl.

(37) Saettel, N. J.; Oxgaard, J.; Wiest, O. *Eur. J. Org. Chem.* **2001**, 1429−1439.
(38) Oxgaard, J.; Wiest, O. *J. Phys. Chem. A* **2001**, *105*, 8236−8240.
(39) Miertuš, S.; Scrocco, E.; Tomasi, J. *Chem. Phys.* **1981**, *55*, 117−129.
(40) Cossi, M.; Scalmani, G.; Rega, N.; Barone, V. *J. Chem. Phys.* **2002**, *117*, 43−54.
(41) Curtin, D. Y. *Rec. Chem. Prog.* **1954**, *15*, 111−128.
(42) Kryachko, E. S.; Nguyen, M. T. *J. Phys. Chem. A* **2001**, *105*, 153−155.
(43) Gold, V.; Satchell, D. P. N. *J. Chem. Soc.* **1955**, 3619−3622.

TABLE 1. Activation Parameters and Energies (kcal/mol) for C−C Bond-Forming Transition States of the Arenium Cation Mechanism in the *o*-Terphenyl Condensation

TS description	$\Delta G^{\ddagger}$ C−C bond-forming step	ΔG relative acidities of corresponding protonation sites	$G^{\ddagger}$ relative to the most stable tautomer
29t: trans,ortho protonation	14.2	0.2	14.4
29c: cis,ortho protonation	19.1	0.2	19.3
36t: trans,para protonation	11.8	0	11.8
36c: cis,para protonation	17.9	0	17.9

The formation of triphenylene requires loss of H_2 after C−C bond formation and deprotonation. As in the case of proton transfer discussed above, the exact nature of this step is unclear, and therefore, calculations were not attempted. Rather, a reasonable value for the activation barrier was assigned based on prior experimental and computational work. The experimental gas-phase activation barrier of the uncatalyzed dehydrogenation of 1,4-cyclohexadiene is 43.8 kcal/mol.[44] The measured condensed phase activation barrier for the oxidative dehydrogenation of 1,4-dihydronaphthalene by 1,4-benzoquinone in ethoxybenzene is 18.9 kcal/mol.[45] Oxidative dehydrogenation by quinones is faster when the product is aromatic.[46] The enthalpy of activation for dehydrogenation of 9,10-dihydroanthracene by acidified nitrobenzene is 6.8 kcal/mol[47]—both $\Delta G^{\ddagger}$ and $\Delta H^{\ddagger}$ of oxidation were set to this value. Oxidation of 1,2-dihydroaromatics should be easier than of 1,4-dihydroaromatics, if concerted. We have conservatively assumed the barrier to dehydrogenation to be 6.8 kcal/mol.

The dehydrogenation of 2,3-dihydrotriphenylene with loss of H_2 is calculated to be exergonic by −27.4 kcal/mol. Dehydrogenation will be more exergonic when coupled with oxidation process, e.g., *p*-quinone + H_2 → hydroquinone reaction, which is calculated to be exergonic by −31 kcal/mol at the same level of theory. Since the oxidant and its product of reaction with hydrogen appear in the net equation of the Scholl reaction, the oxidant strength influences the net energetics of the reaction. The oxidant strength will affect the relative energies of the dihydroaromatic and fully benzenoid intermediates or products. In the case of multistep reactions this becomes more interesting, as the oxidant strength may shift the position of the rate-determining transition state toward the final product (see C_6Ph_6 section).

The fair comparison of the arenium cation and the radical cation mechanism for the conversion of *o*-terphenyl to triphenylene requires judicious choice of both the acid and the oxidant. To accomplish this, we chose reagents in such way that the initial step for both reactions, protonation or one-electron oxidation, is thermoneutral. Thus, $B\mathrm{H}^+$ = **28** and *O* = oxidant, with the strength such that $\Delta G(O + \mathrm{H_2} \rightarrow O\mathrm{H_2}) = \Delta G(2B + 2\mathbf{11}^{\bullet +} + \mathrm{H_2} \rightarrow 2B\mathrm{H}^+ + 2\mathbf{11})$. The complete thermochemical argument is included in the Supporting Information.

In the case of the trans transition state geometry and ortho protonation, the C−C bond-forming activation barrier was calculated to be 14.2 kcal/mol, and the step was endergonic, +4.7 kcal/mol. This compares to a 11.8 kcal/mol barrier and a 8.1 kcal/mol endergonicity for trans geometry and para protonation (Scheme 5). Pathways leading to cis products result in higher activation energies: 19.1 kcal/mol (ortho protonation) and 17.9 kcal/mol (para protonation), and higher endergonicities: +9.9 kcal/mol (ortho) and +13.4 kcal/mol.

Again, the Curtin−Hammett principle[41] applies—neither simple comparison of the basicities of different protonation sites in tautomers **28** (ortho) or **35** (para), nor comparison the activation barriers for C−C bond formation from **28** and **35**, is appropriate. Rather, the absolute values of the corresponding C−C bond forming transition state energies define the preferred reaction pathway. Table 1 summarizes these parameters for the four C−C bond-forming TS shown in Scheme 5. The transition state resulting from para protonation with a trans geometry, **36t**, is preferred, followed closely by **29t**.

***o*-Terphenyl Coupling: Radical Cation Mechanism.** Cyclization of the *o*-terphenyl radical cation was considered next. Its formation would require use of a strong oxidant—the *o*-terphenyl ionization potential from photoelectron spectroscopy is 7.99 eV[48] and the $E^{\circ x}_{1/2}$ is +1.30 V vs $\mathrm{Ag|Ag^+}$ in acetonitrile.[49] As was the case for the protonation mechanism, two geometries (trans and cis) were considered. Cyclization of the *o*-terphenyl radical cation **42** to give the trans isomer **44t** was calculated to be endergonic by 23.5 kcal/mol and cyclization to give the cis isomer **44c** was calculated to be endergonic by 28.5 kcal/mol.

The thermochemistry of the generation of the *o*-terphenyl radical cation from *o*-terphenyl via electron transfer to a one-electron oxidant can be controlled by choice of the oxidant and reactions conditions. Oxidants strong enough to warrant exergonicity of this process are available, e.g., Ce^{4+}. However, the free energy barriers for both the trans and cis C−C bond-forming steps of the radical cation were substantial: 27.3 and 30.0 kcal/mol, respectively. The structures of these transition states strongly resemble those of the cyclized radical cation products, to which they are also close in energy (very small barriers for reverse reactions), providing an illustration of the Hammond postulate. Calculations at the BHandHLYP/6-31G-(d) level provide similar results, with slightly lower free energy expenditure (21.6 kcal/mol) and barrier (25.3 kcal/mol) to C−C bond formation predicted (trans geometry).

Identifying the nature of the Scholl reaction—arenium cation or radical cation — is an objective of this work. As mentioned before, these fundamentally different mechanisms can be directly compared if the acid and oxidant are chosen to provide the identical net energetic outcome for both reactions. The use of protonated *o*-terphenyl as an acid ($B\mathrm{H}^+$) and the radical cation of *o*-terphenyl as oxidant (*O*) satisfy this criterion. Side-by-side reaction coordinate diagrams with these thermodynamic assumptions are presented in Figure 1.

(44) (a) Rico, R. J.; Page, M.; Doubleday, C., Jr. *J. Am. Chem. Soc.* **1992**, *114*, 1131−1136. (b) Benson, S. W.; Shaw, R. *Trans. Faraday Soc.* **1967**, *63*, 985−992.

(45) Braude, E. A.; Jackman, L. M.; Linstead, R. P. *J. Chem. Soc.* **1954**, 3548−3563.

(46) Stoos, F.; Roček, J. *J. Am. Chem. Soc.* **1972**, *94*, 2719−2723.

(47) Cristiano, M. L. S.; Gago, D. J. P.; Gonsalves, A. M., d'A. R.; Johnstone, R. A. W.; McCarron, M.; Varejão, J. M. T. B. *Org. Biomol. Chem.* **2003**, *1*, 565−574.

(48) Dewar, M. J. S.; Goodman, D. W. *J. Chem. Soc., Faraday Trans. 2* **1972**, *68*, 1784−1788.

(49) Mizuno, K.; Ichinose, N.; Tamai, T.; Otsuji, Y. *Tetrahedron Lett.* **1985**, *26*, 5823−5826.

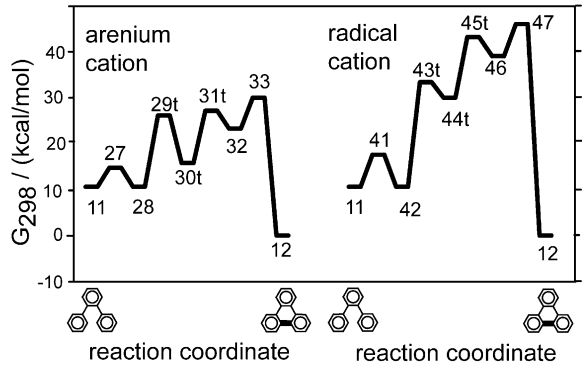

FIGURE 1. Comparison of reaction coordinates.

The key difference between the arenium cation mechanism and the radical cation mechanism is that the cyclized Wheland intermediate **37t** (and its analogues) is much lower in energy (~15 kcal/mol) than the cyclized radical cation **44t** (and its analogues) (Scheme 6). This difference is also manifest in the corresponding deprotonated forms **39/32** and **46**. Since these intermediates define the rate-determining proton transfer and oxidation barriers, the arenium cation mechanism appears to be favored.

1,2,3-Triphenylbenzene: Arenium Cation Mechanism. In 1,2,3-triphenylbenzene, **48**, two aryl−aryl bonds must be formed to produce dibenzo[*fg*,*op*]naphthacene **71** (Scheme 7). We expect that 1-phenyltriphenylene **56** is the fully benzenoid intermediate in this process. Since the dihydro intermediate is much higher in energy relative to the fully benzenoid product + H_2, deprotonation and oxidation to restore aromaticity will precede formation of the second C−C bond. If this were not the case, the simultaneous loss of aromatic stabilization in multiple benzene rings would be energetically unreasonable.

Since in larger systems the consideration of all transition-state possibilities becomes prohibitively time-consuming, only trans transition-state geometries, which were the most favorable for *o*-terphenyl, were calculated. Different sites of initial protonation were considered to ensure that Curtin−Hammett scenarios were properly modeled.

We now adopt the thermodynamic standard of loss of H_2; e.g., no oxidant is used. This is the equivalent of reporting energies with respect to a standard hydrogen electrode. We continue to use reference acid that provides a thermoneutral first proton-transfer step. For para protonation, formation of the first aryl−aryl bond requires overcoming an 11.2 kcal/mol free energy barrier and is endergonic by 5.9 kcal/mol. For ortho protonation, formation of the first aryl-aryl bond requires overcoming a 13.4 kcal/mol energy barrier and is endergonic by 5.8 kcal/mol. These calculated free energy barriers are about 0.7 kcal/mol lower than the barriers for analogous *o*-terphenyl geometries, indicating that the additional phenyl group stabilizes the transition states relative to the protonated hydrocarbon.

The formation of the second C−C bond, the conversion of **56** to **71**, involves more possible protonation sites. To examine influence of the choice of the protonation sites, two series were considered: phenyl group protonation ortho and para relative to the nascent bond (i.e., **64** and **72**) and triphenylene core protonation ortho and para relative to the nascent bond (i.e., **79** and **86**). Protonation of the phenyl group results in remarkably low free energy activation barriers to CC bond formation, 6.3 and 8.4 kcal/mol for para and ortho protonation, respectively, and the reaction becomes exergonic: −1.6 (para) and −4.5 kcal/mol (ortho). In contrast, when the triphenylene fragment is protonated, activation barriers rise to 16.0 and 20.5 kcal/mol (para and ortho, respectively) and reaction is endergonic: 9.8 (para) and 4.6 kcal/mol (ortho) (Figure 2).

SCHEME 6. Radical Cation Mechanism for *o*-Terphenyl

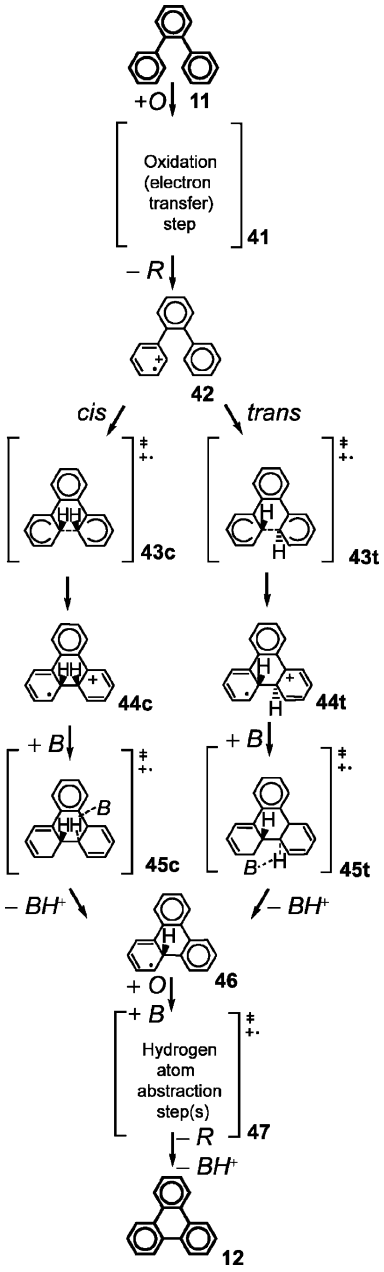

However, the triphenylene moiety is much more basic than the phenyl group, presumably because the resulting charge is more delocalized. Ortho protonation of the triphenylene moiety to give cation **80** results in a structure 14.7 kcal/mol more stable (ΔG) than ortho protonation at the phenyl group to give cation **65**. Once again, the Curtin−Hammet principle applies: para protonation of the triphenylene moiety gives the lowest energy C−C bond-forming TS (Table 2).

The results for 1,2,3-triphenylbenzene indicate that introduction of the second ary-aryl bond by the arenium cation mechanism will be easier than formation of the first. Since the pathways intersect at the fully benzenoid intermediate **56**, the actual pathway is probably a combination of the pathways shown. The two most favorable pathways are shown in Figure 2.

SCHEME 7. Arenium Cation Mechanisms for Condensation of 1,2,3-Triphenylbenzene

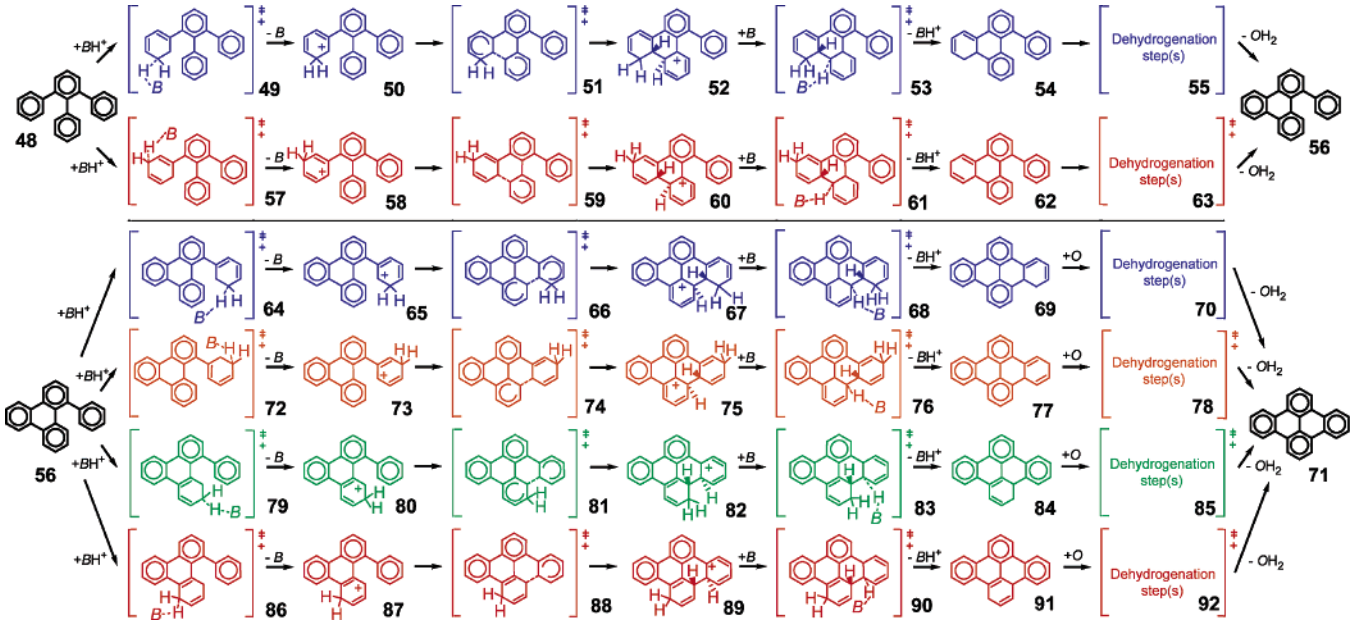

TABLE 2. Activation Parameters for the Arenium Cation Mechanism in 1-Phenyltriphenylene (kcal/mol) (Scheme 7)

TS	$\Delta G^{\ddagger}$, C−C bond-forming step, relative to **65, 73, 80, 87**	ΔG, acidities of protonation sites, relative to **87**	$G^{\ddagger}$, relative to the most stable tautomer
o-phenyl protonation, **66**	8.4	14.8	23.3
p-phenyl protonation, **74**	6.3	14.1	20.4
o-triphenylene protonation, **81**	20.5	0.2	20.7
p-triphenylene protonation, **88**	16.0	0.0	16.0

1,2,3-Triphenylbenzene: Radical Cation Mechanism. The radical cation mechanism was disfavored with respect to the arenium mechanism in the condensation of *o*-terphenyl. To determine if the radical pathway is increasingly favored in larger systems, this mechanism was examined in condensation of 1,2,3-triphenylbenzene (Scheme 8).

Both trans and cis geometries were considered for the formation of the first C−C bond (**95t** and **95c**), the former resulting in 30.0 kcal/mol free energy barrier and 27.4 kcal/mol endergonicity (full convergence of geometry of **96t** could not be achieved), the latter yielding 29.3 kcal/mol barrier and 28.1 kcal/mol endergonicity. These numbers indicate that the radical cation mechanism in the C−C bond formation step requires overcoming barriers larger than in the worst considered case of the arenium cation mechanism. The formation of the second C−C bond, **56** → **71** via **102**, was also investigated. The activation barrier and endergonicity remained high, at 24.2 and 20.3 kcal/mol, respectively. It is unlikely that radical cation mechanism is feasible for either *o*-terphenyl or 1,2,3-triphenylbenzene. Our thermochemistry data for **94**, **95t** and **96t** are in good agreement with the B3LYP/3-21G calculations by Di Stefano et al. published recently on *o*-terphenyl radical cation.[20]

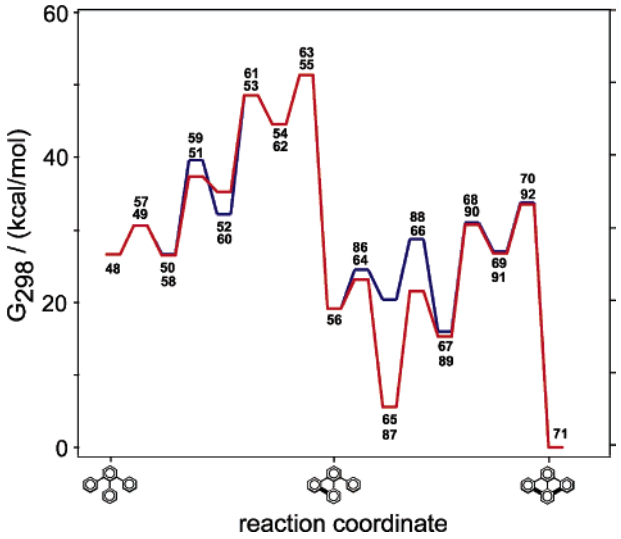

FIGURE 2. Reaction profiles for the most favorable arenium cation mechanisms described in Scheme 7.

1,2,3,4-Tetraphenylbenzene: Arenium Cation Mechanism. The computational results for *o*-terphenyl and 1,2,3-triphenylbenzene suggest the following two mechanistic pathways merit consideration. In the first pathway, the phenyl group adjacent to the developing PAH system is protonated ortho to the new bond and C−C bond formation occurs via a trans geometry. Deprotonation and dehydrogenation follow. Next, the phenyl group adjacent to the growing PAH core is protonated and the cycle continues. Ortho protonation was chosen, as it consistently results in largest exergonicity (lowest endergonicity) of the CC bond-forming reaction, although activation barriers are lower for para protonation. The second pathway differs from the first in that the growing PAH system is protonated. Both pathways are illustrated in Scheme 9.

The first C−C bond-forming step in the condensation of 1,2,3,4-tetraphenylbenzene (**107**) in the ortho protonation pathway requires 13.4 kcal/mol $\Delta G^{\ddagger}$ (**110**) and is endergonic by

SCHEME 8. Radical Mechanism for the Condensation of 1,2,3-Triphenylbenzene

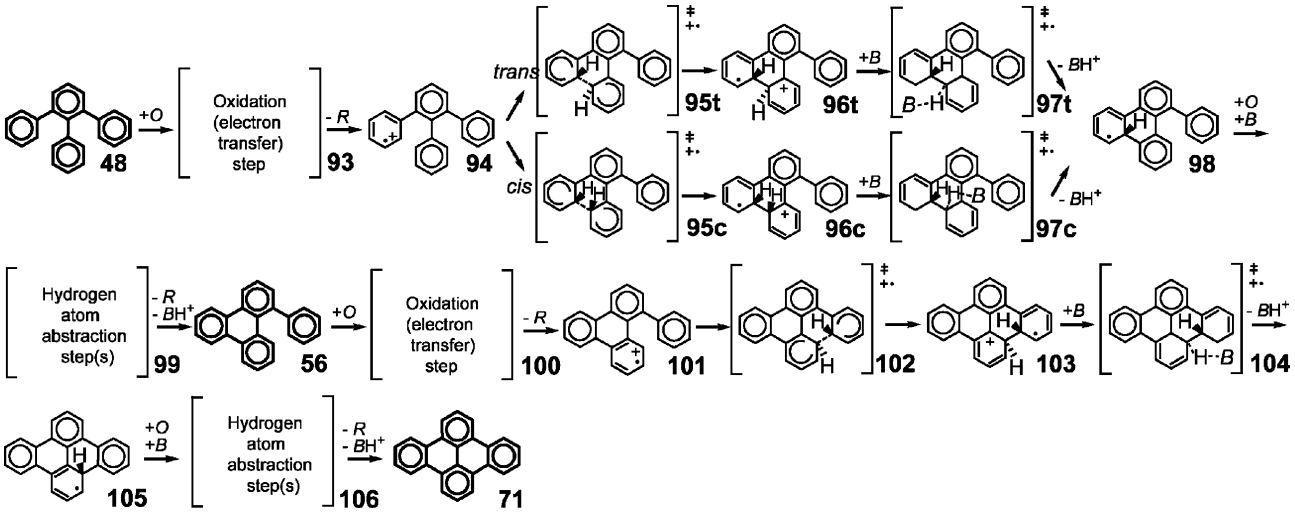

SCHEME 9. Stationary Points on the *o*-Phenyl Protonation (Blue) and *p*-PAH Protonation (Red) Pathways for Arenium Cation Condensation of 1,2,3,4-Tetraphenylbenzene

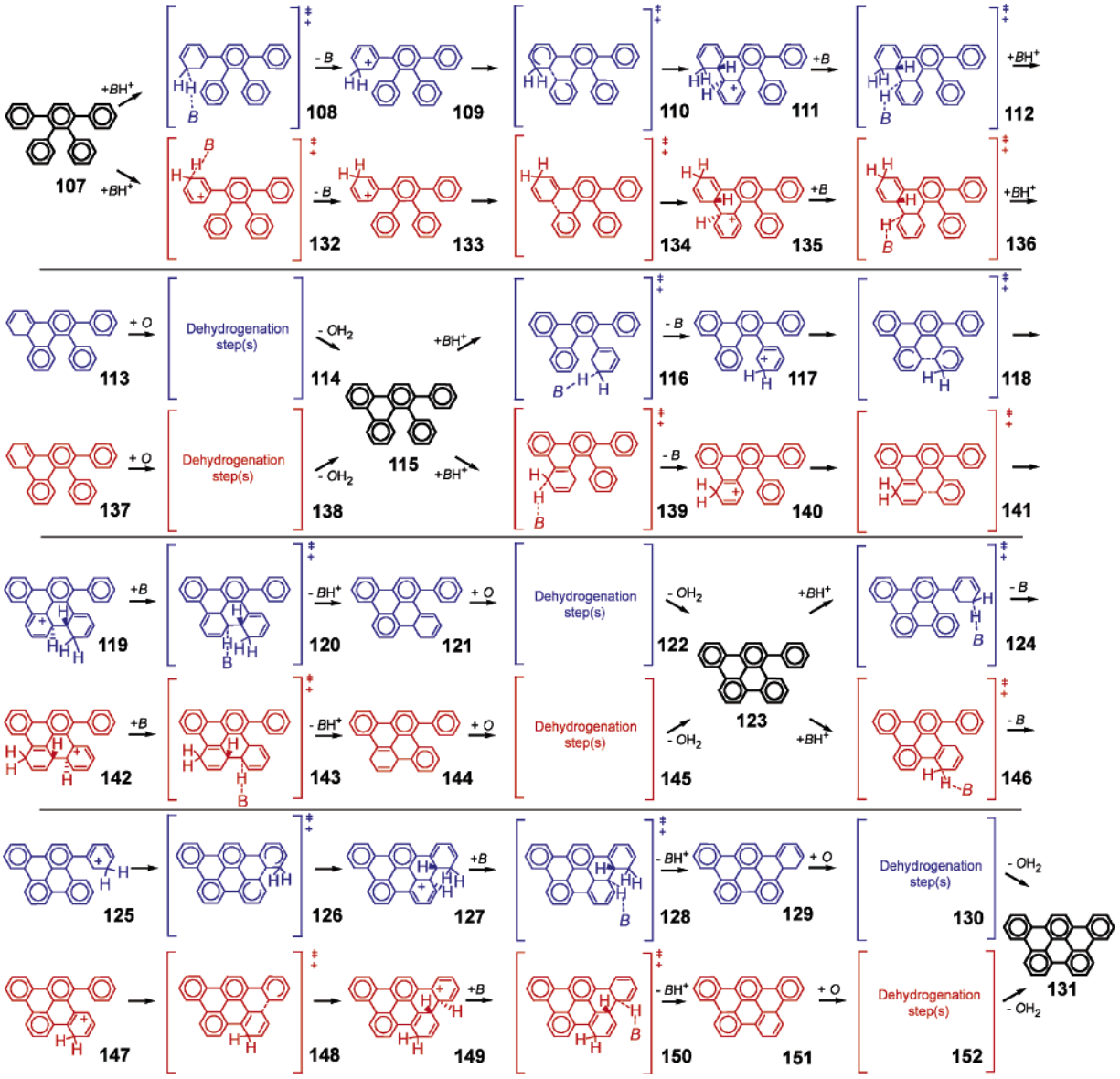

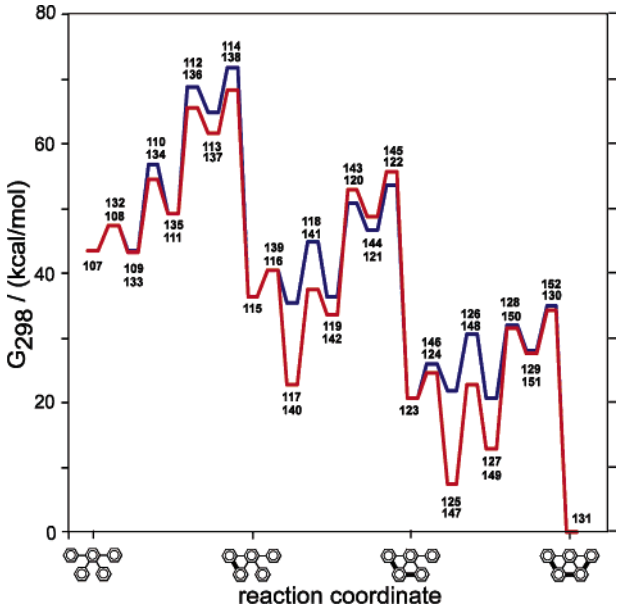

FIGURE 3. Reaction profiles for mechanisms described in Scheme 11. BH^+ = **109**, *O* = none, free H_2 evolution.

5.8 kcal/mol. This is consistent with results obtained for *o*-terphenyl and 1,2,3-triphenylbenzene.

Figure 3 compares reaction profiles for the *o*-phenyl and *p*-PAH protonation mechanisms with the thermodynamic assumptions that H_2 is evolved and protonated 1,2,3,4-tetraphenylbenzene, **109** (or acid of identical strength), serves as an acid. This figure indicates that either the dehydrogenation TSs (**114**, **138**) or the deprotonation TSs (**112**, **136**) immediately after the formation of the first C−C bond is rate determining. Because common intermediates are involved, the actual optimal pathway could be a combination of the *o*-phenyl protonation and the *p*-PAH protonation pathways.

It is noteworthy that the first complete Scholl step (**107** to **115)** is thermoneutral, while subsequent condensations (**115** to **123** and **123** to **131)** are exergonic. A similar pattern is observed for C_6Ph_6 and we believe that this phenomenon has major consequences for the course of this type of reactions.

Hexaphenylbenzene: Arenium Cation Mechanism. The ultimate goal of this study is consideration of the condensation of C_6Ph_6 to HBC. The same mechanistic schemes described for 1,2,3,4-tetraphenylbenzene were applied to this reaction: *o*-phenyl protonation with trans C−C bond formation and para protonation of the PAH core (initially a phenyl group) with trans

SCHEME 10. Stationary Points on the *o*-Phenyl (Blue) Pathway for the Arenium Cation Condensation of C_6Ph_6 to HBC

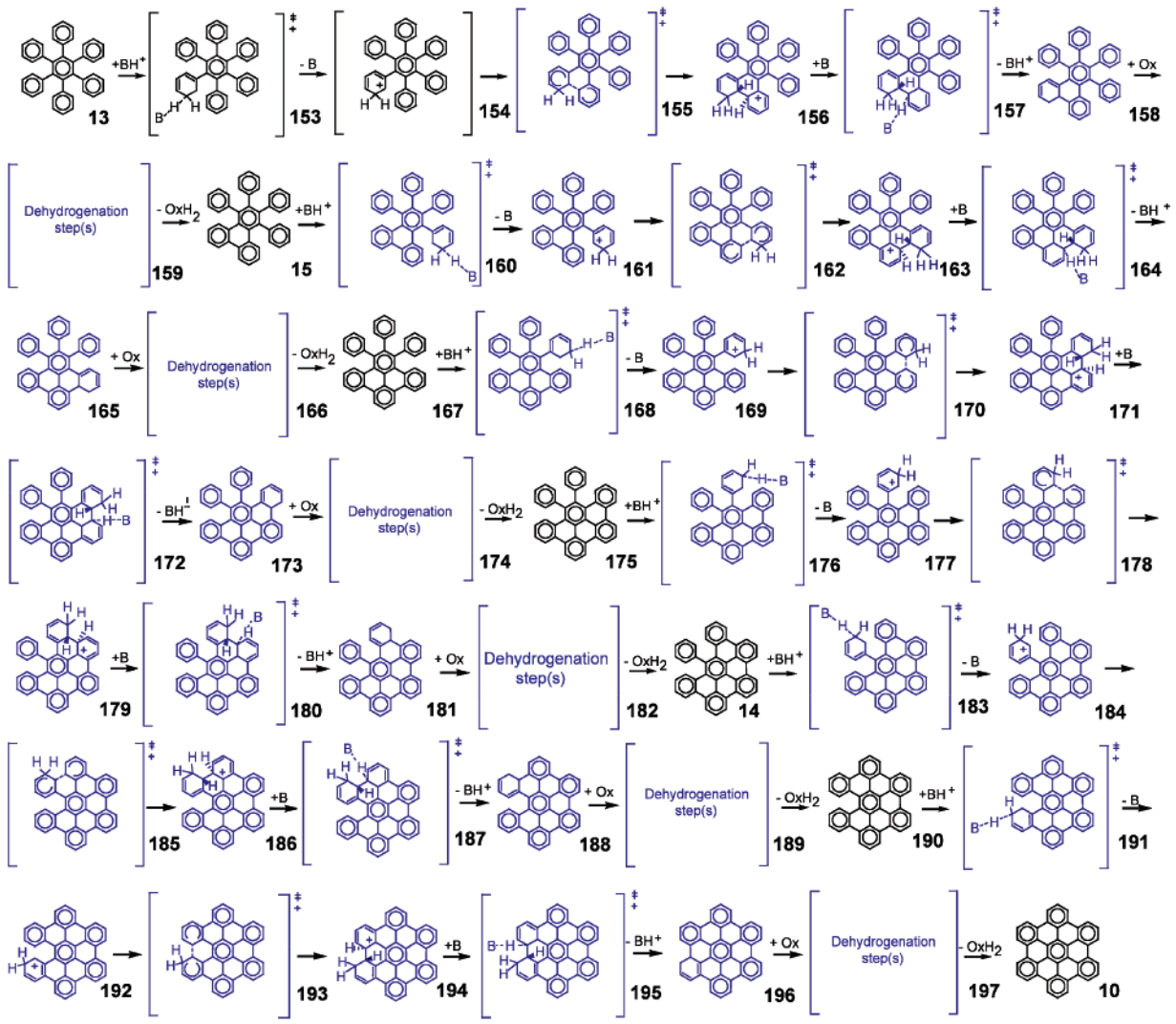

SCHEME 11. Stationary Points on the *p*-PAH Protonation Pathway (Red) for the Arenium Cation Condensation of C_6Ph_6 to HBC

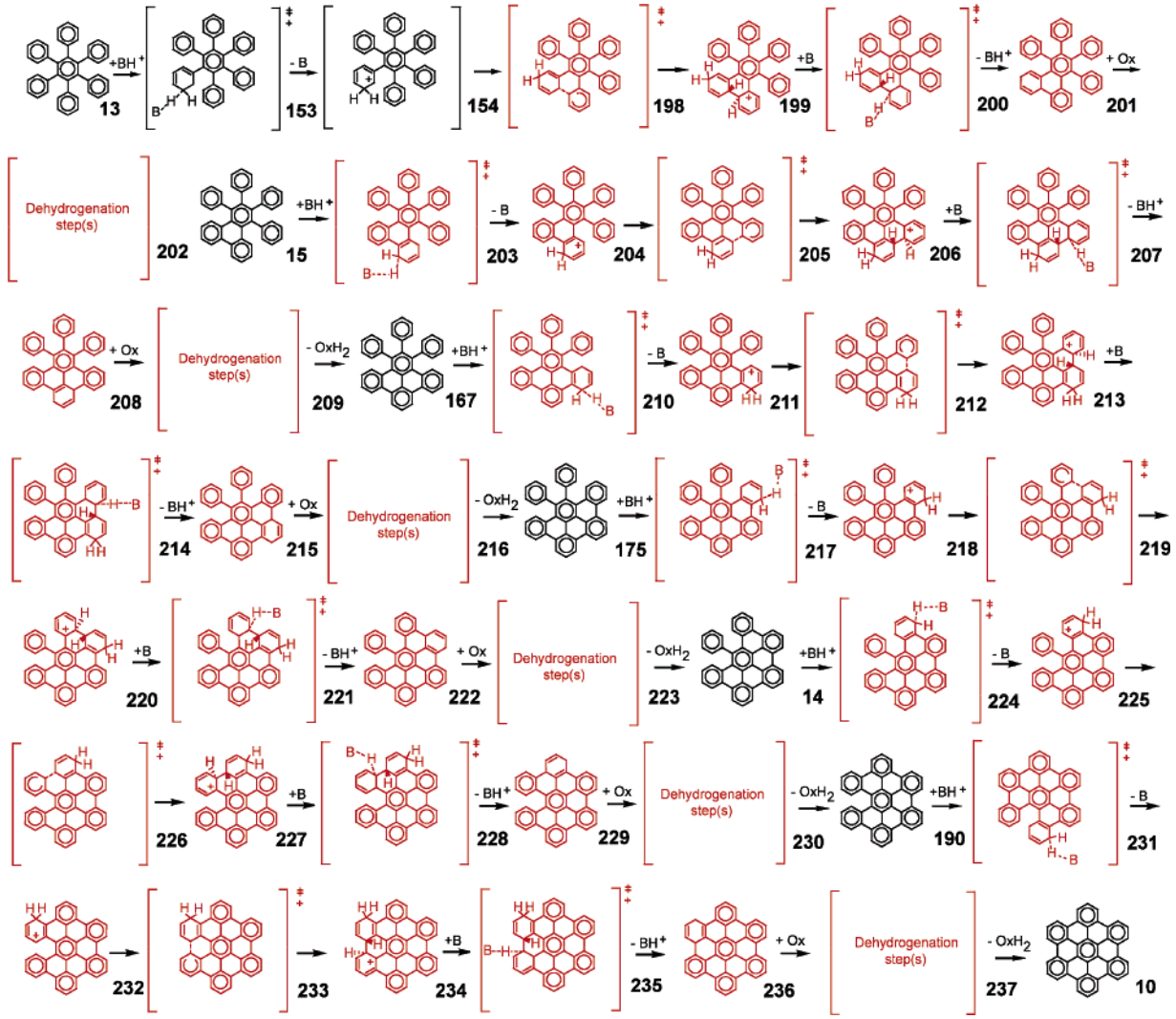

C−C bond formation. The results are summarized in Schemes 10 and 11 and Figure 4.

An optimal combination of two pathways, as common intermediates are present, can be chosen. Table 3 shows, for both pathways, the energies of highest transition states, relative to the proceeding fully benzenoid compound, for each of the six bonds formed. These data indicate that the formation of the first and last three bonds formation will follow the *o*-phenyl protonation pathway, while the second and third aryl-aryl bond formation will follow the *p*-PAH pathway. The oxidation step in the formation of the first C−C bond will be rate determining ($\Delta G^{\ddagger}_{rel}$, 21.4 kcal/mol); the subsequent cyclizations will be faster ($\Delta G^{\ddagger}_{rel}$ < 17 kcal/mol). The overall reaction is exergonic by −93.8 kcal/mol, which is −15.6 kcal/mol/C−C bond, assuming hydrogen evolution (no oxidant).

The dehydrogenation steps become more exergonic with the progress of the reaction—this can be attributed to the increasing electron delocalization in the intermediates, all of which are fully benzenoid. This increasing exergonicity can be related to the increasing resonance energy per π electron (REPE)[50] of the growing PAH core (3.43, 3.53, 3.55, 3.50, 3.63 kcal/mol for triphenylene, dibenzonaphthacene, tribenzoperylene, dibenzophenanthropentaphene (cf. benzene, 3.34 kcal/mol)).[50] We propose, as before,[1] that this "slippery slope" phenomenon is responsible for the success of the Scholl condensation of dendritic oligophenylenes.

The stereochemistry of the fully benzenoid intermediates (e.g., **15, 167,** etc.) merits discussion. While the *o*-phenyl protonation pathway leads to C_2-symmetrical benzenoid intermediates, the *p*-PAH protonation pathway leads to C_s symmetrical benzenoid intermediates. The fully benzenoid intermediates **14** and **190** are exceptions—the C_2 structure is preferred in both cases. Nonetheless, energy differences between C_2 and C_s structures are low, and they are most likely in rapid equilibrium. To keep the two pathways readily comparable, the C_2 geometries were used in both schemes.

Other pathways may exist—the formation of C−C bonds is not necessarily contiguous. To examine this possibility, the strain energy of all fully benzenoid minima on the potential energy surface for the conversion of C_6Ph_6 to HBC were calculated (Scheme 12). Strain was defined by a homodesmotic reaction with triphenylene and *o*-terphenyl as unstrained references. Indeed, the least strained intermediates lie on the contiguous pathway, supporting the contiguous formation of C−C bonds.

(50) Randić, M.; Guo, X. *New J. Chem.* **1999**, *23*, 251−260.

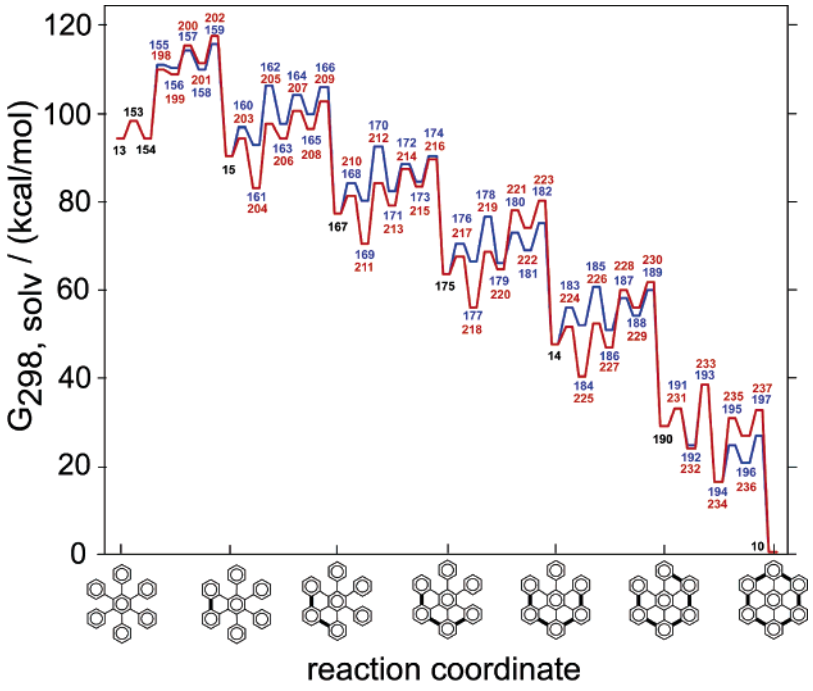

FIGURE 4. Energetics comparison of the *o*-phenyl protonation (blue) and *p*-PAH protonation (red) pathways of the condensation of C_6Ph_6 to HBC. Acid = 154, H_2 evolution.

TABLE 3. Maximum Free Energy TSs between Fully Benzenoid Compoundsa

	ortho pathway		*p*-PAH pathway	
bond formation	$G^{\ddagger}_{rel}$, kcal/mol	structure	$\Delta G^{\ddagger}_{rel}$, kcal/mol	structure
1	21.4	**159**	22.9	**202**
2	15.7	**166**	12.2	**209**
3	15.3	**170**	12.2	**216**
4	13.2	**178**	16.7	**223**
5	12.9	**189**	14.2	**230**
6	9.2	**193**	9.4	**233**

[a] The lowest energy TS for each step is underlined.

Of course, TS barriers determine the favored reaction pathway, but these are likely to be related by the relative energies of the fully benzenoid intermediates.

It is interesting to notice that the strain in the proposed scheme generally decreases with the number of C−C bonds. The strain actually becomes negative for **190** and **10.** This indicates that electronic stabilization due to increased delocalization is not taken into account in our definition of strain.

The influence of the catalytic acid is easily understood (Figure 5). The relative energies of the neutral species are not affected by choice of the acid. A weak acid will render the key protonated intermediates inaccessible. A very strong acid would cause the protonated intermediates to become energetic sinks, which would slow the formation of the dihydro precursors.

The more complex role of the oxidant is revealed by Figure 6. A weak oxidant not only lowers overall exergonicity, but can shift the position of the rate determining transition state. As a consequence, a weak oxidant would be beneficial if partially condensed intermediates are desired.

Synthetic Study and Kinetic Modeling. The exceedingly low solubility of HBC hinders the experimental investigation of its formation from C_6Ph_6. However, analysis of the end reaction mixture provided some mechanistic insight.

The rate-determining TS is the oxidation (**159**, **202**, Schemes 10 and 11, Figure 4), or possibly the proton transfer, following the first C−C bond formation. Regardless of the exact nature of this TS, it is clear that the rate-determining TS[51] occurs in the course of the formation of the first C−C bond. It follows that the intermediates should not accumulate during the course of the reaction: after the formation of the first C−C bond, all intermediates will be consumed faster than they are formed. Moreover, each step is increasingly exergonic. This observation, together with the Hammond postulate, implies that each cyclization will be faster than the preceding one.

Simulation[52] of a simplified kinetic scheme, which involves only the fully benzenoid hydrocarbons and the highest energy transition states of the lowest energy pathway (Table 3), supports this analysis. A preexponential factor of 10^{11} M^{-1} s^{-1} was used. The simulation, based on 1 mM C_6Ph_6, 6 mM oxidant, and excess acid, suggests that no intermediates will accumulate in quantities exceeding 5×10^{-8} M (Figure 7).

Analytical treatment of a simple irreversible model, $A_1 \rightarrow A_2 \rightarrow A_3$, with rate constants k_1 and k_2, and $[A_1]_{t=0} = [A_1]_0$, $[A_2]_{t=0} = [A_3]_{t=0} = 0$, offers some insight to why intermediates do not accumulate. This scheme would describe the condensation of 1,2,3-triphenyl benzene in the presence of an excess of acid and oxidant. The analytical solution for the concentration of intermediate A_2 is $[A_2] = [A_1]_0k_1(e^{-k_1t} - e^{-k_2t})/(k_2 - k_1)$. Keeping k_1 constant and varying k_2 from ∞ to 0, $[A_2]_{max}$, the maximum concentration of the intermediate A_2, spans a range from 0 to $[A_1]_0$, as expected. For the case $k_2 = k_1$, $[A_2]_{max}$ equals $[A_1]_0/e$ at $t_{max} = k_1^{-1} = k_2^{-1}$. As the first step becomes rate limiting ($k_2 > k_1$), $[A_2]_{max}$ not only decreases, but the peak concentration occurs earlier. If k_2 and k_1 are governed by Arrhenius behavior and their preexponential factors are equal,

(51) Espenson, J. H. *Chemical Kinetics and Reaction Mechanisms*, 2nd ed.; McGraw-Hill: New York, 1995.

(52) *Chemical Kinetics Simulator*; Chemical Kinetics Simulator v. 1.01, IBM Corp., 1996.

SCHEME 12. Possible Pathways Connecting Benzenoid Intermediates in Condensation of C_6Ph_6

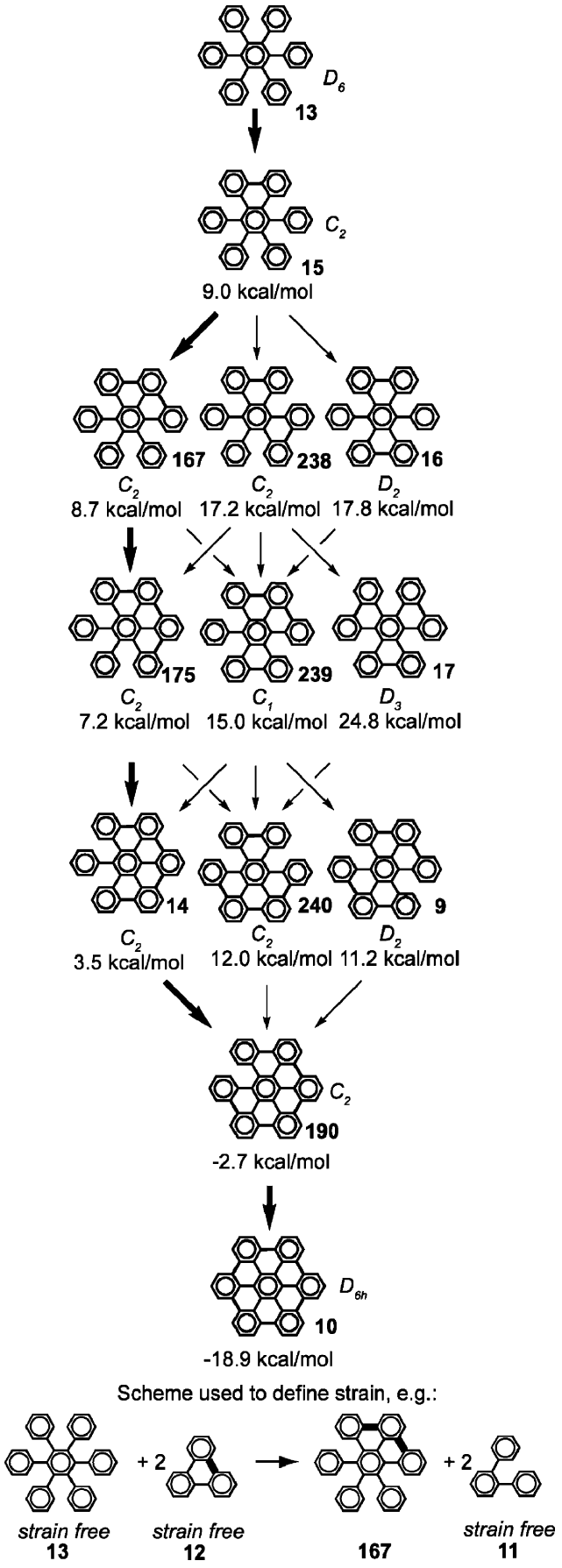

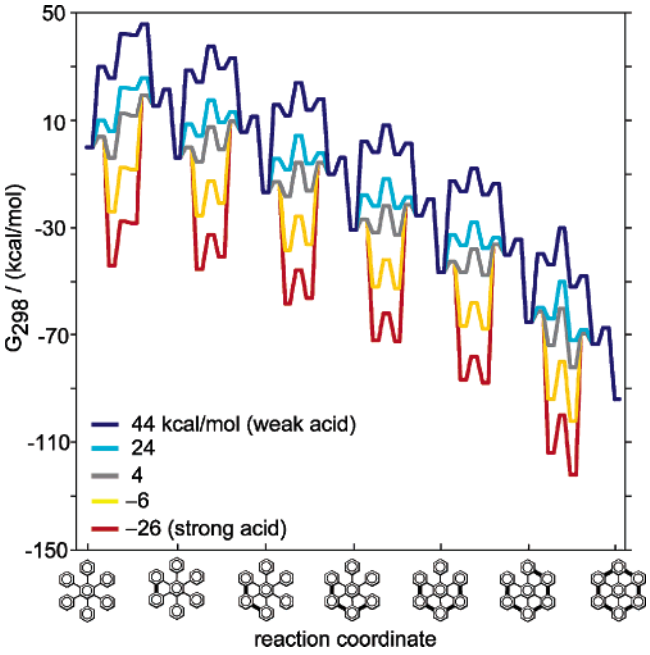

FIGURE 5. Influence of the acid strength (defined as $\Delta_r G$ ($BH^+_{(sol)} + T_{(sol)} \rightarrow B_{(sol)} + TH^+_{(sol)}$), T = terphenyl).

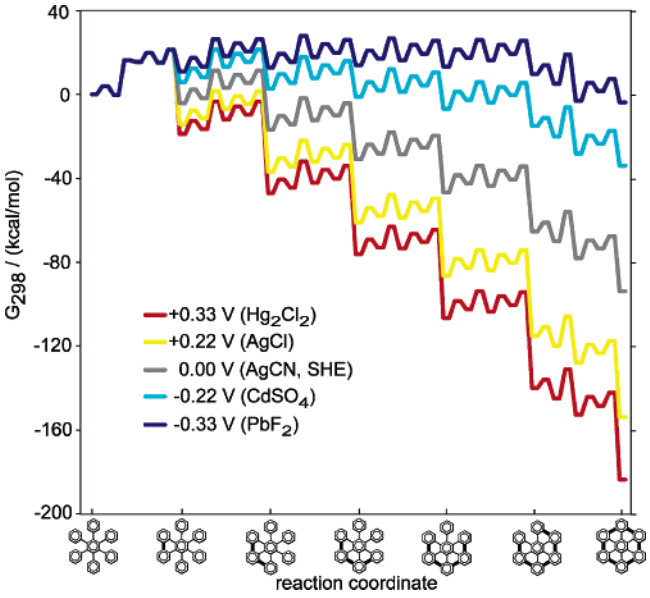

FIGURE 6. Influence of the oxidant strength (defined as $\Delta_r G$ ($O_{(sol)} + H_{2(sol)} \rightarrow OH_{2(sol)}$)).

a 2 kcal/mol difference in activation energy at 298 K, i.e., $E_2^{\ddagger} - E_1^{\ddagger} = -2$ kcal/mol would make k_2 faster than k_1 by a factor 30. This would result in the maximum concentration of A_2 being only 3% of $[A_1]_0$.

Another interesting system is based on the sequence of second-order irreversible processes: a + o → b + r, b + o → c + r, c + o → d + r, ..., f + o → g + r, where o = oxidant, r = reduced form, $[a]_{t=0} = 1$, and $k_1 = k_2 = ... = k_6$. Both numerical solutions of the differential equations and stochastic simulation of this reaction system demonstrate that the initial concentration of the oxidant $[o]_{t=0}$ determines the distribution of the intermediates and the final product at $t \rightarrow \infty$ (Figure 8). Interestingly, the maximum concentration of the intermediate "e" is achieved when $[o]_{t=0} = 4.0$, which is the stoichiometric

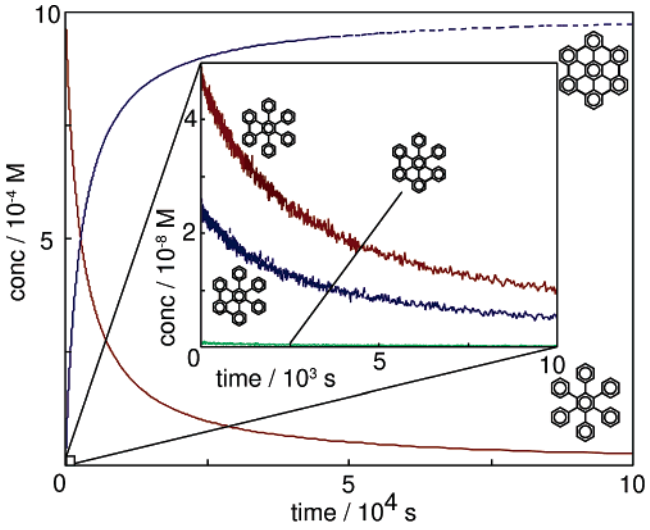

FIGURE 7. Concentrations of important species from kinetic simulations.

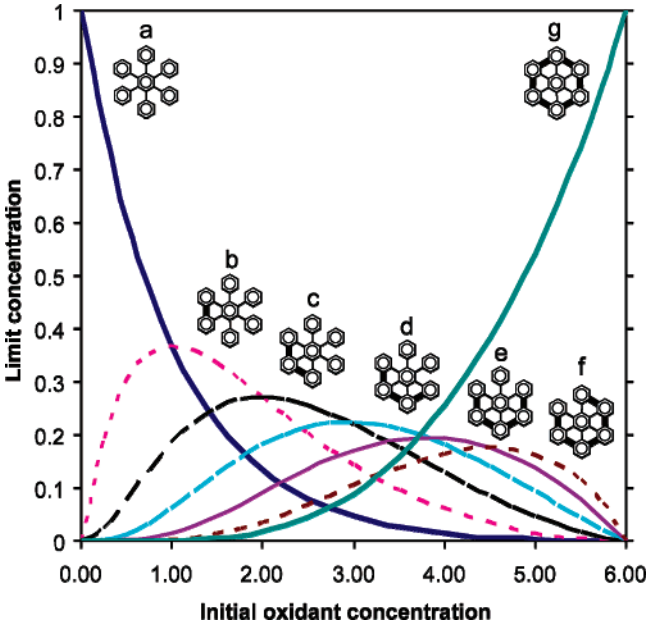

FIGURE 8. Ultimate ($t \rightarrow \infty$) concentrations as a function of initial concentration assuming a sequence of irreversible steps without a rate-limiting step.

ratio for formation of "e" (this also applies to other intermediates). This intermediate "e" corresponds to compound **14** reported by Müllen and co-workers.[18]

These mathematical models and simulations show that small reductions in the activation energy of the consecutive steps limit accumulation of intermediates. The progressive lessening of activation barriers—the slippery slope effect—has two implications: (1) many consecutive reactions occur readily and (2) intermediates will not accumulate. Consecutive intermediates show decreasing maximum concentrations (Figure 7), as expected for a scheme in which the first step is rate determining.

To test these predictions, a series of experiments were performed in which the quantity of oxidant was varied and reaction mixtures were carefully analyzed. Several oxidizing systems were investigated: $MoCl_5$ in CH_2Cl_2 at rt[53−59] (entries 1−4), $PhI(O_2CCF_3)_2/BF_3{\cdot}Et_2O$ in CH_2Cl_2 at −40 °C[60] (entries 5−8), $CuCl_2$ with $AlCl_3$ in CS_2 at rt[18] (entries 9−11), $Cu(OTf)_2$ with $AlCl_3$ in CS_2 at rt (entry 12), and $FeCl_3$ in CH_2Cl_2 at rt[17,61] (entry 14). The variable stoichiometry oxidations are summarized in Table 4. In all cases except entry 13, mass balances were nearly quantitative (Figure 9).

TABLE 4. Oxidation of C_6Ph_6 to HBC

trial	mole ratio oxidant/HBC	yield HBC (%)	recovered C_6Ph_6 (%)
	$MoCl_5$ in CH_2Cl_2		
1	0.97	6.0	94.2
2	3.0	41.5	54.8
3	6.0	68.8	28.6
4	12	99.3	2.3
	$PhI(O_2CCF_3)_2/BF_3{\cdot}Et_2O$ in CH_2Cl_2		
5	1.0	5.3	86.9
6	3.0	34.7	71.0
7	5.9	81.1	23.6
8	9.0	77.8	8.0
	$CuCl_2$ /$AlCl_3$ in CS_2		
9	1.0	6.9	91.9
10	6.0	18.8	76.2
11	12	60.3	33.1
	$Cu(OTf)_2/AlCl_3$ in CS_2		
12	6.0	0.0	90.3
	$FeCl_3$ in CH_2Cl_2		
13[a]	18	117.7	30.0

[a] Intractable mixture.

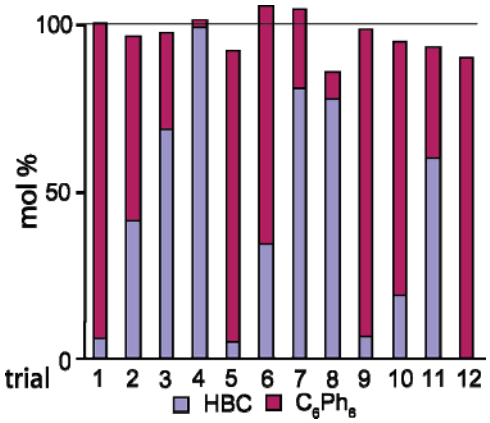

FIGURE 9. Mass balance summary (Table 4).

$MoCl_5/CH_2Cl_2$ is a homogeneous medium for the Scholl reaction[57,62] and converts C_6Ph_6 to HBC in good yield. A disadvantage of this reagent is that chlorinated impurities are formed, as indicated by MALDI-TOF MS and combustion analyses of the crude product.

(53) Kumar, S.; Manickam, M. *Chem. Commun.* **1997**, 1615−1616.
(54) Waldvogel, S. R.; Wartini, A. R.; Rasmussen, P. H.; Rebek, J., Jr. *Tetrahedron Lett.* **1999**, *40*, 3515−3518.
(55) Waldvogel, S. R.; Fröhlich, R.; Schalley, C. A. *Angew. Chem., Int. Ed. Engl.* **2000**, *39*, 2472−2475.
(56) Waldvogel, S. R. *Synlett* **2002**, 622−624.
(57) Waldvogel, S. R.; Aits, E.; Holst, C.; Fröhlich, R. *Chem. Commun.* **2002**, 1278−1279.
(58) Kramer, B.; Averhoff, A.; Waldvogel, S. R. *Angew. Chem., Int. Ed.* **2002**, *41*, 2981−2982.
(59) Kramer, B.; Fröhlich, R.; Bergander, K.; Waldvogel, S. R. *Synthesis* **2003**, 91−96.
(60) Takada, T.; Arisawa, M.; Gyoten, M.; Hamada, R.; Tohma, H.; Kita, Y. *J. Org. Chem.* **1998**, *63*, 7698−7706.
(61) Fechtenkötter, A.; Tchebotareva, N.; Watson, M.; Müllen, K. *Tetrahedron* **2001**, *57*, 3769−3783.
(62) Kovacic, P.; Lange, R. M. *J. Org. Chem.* **1963**, *28*, 968−972.

Little is known about the stoichiometry or the mechanism of the reaction of $MoCl_5$ with aromatics. It is not fully clear whether the reaction is a two-electron ($Mo^{5+} + 2e \rightarrow Mo^{3+}$; $Mo^{5+} + 2[H] \rightarrow Mo^{3+} + 2H^+$) or one-electron process ($Mo^{5+} + e \rightarrow Mo^{4+}$; $Mo^{5+} + [H] \rightarrow Mo^{4+} + H^+$). Preparation of $MoCl_4$ by reaction of $MoCl_5$ with benzene, where chlorobenzene is generated,[63] was reported. We have isolated $MoCl_3$, which was identified by X-ray crystallography, from the reaction mixture after quenching with methanol. However, the presence of this compound might arise from the reduction of $MoCl_5$ or $MoCl_4$ with methanol.

Cyclodehydrogenation by $PhI(O_2CCF_3)_2/BF_3{\cdot}Et_2O$ is usually performed at low temperatures (−40 °C) for 1.5 h.[60] In our experiments, we extended reaction time to 3.5 h and the temperature was allowed to rise slowly to −10 °C. Good yields of **10** were obtained under these conditions.

Oxidations using $Cu(OTf)_2$, $CuCl_2$, and $FeCl_3$ were performed for comparison. Reactions with $CuCl_2$ for 12 h afforded lower conversions, probably due to its low solubility in CS_2. $Cu(OTf)_2$ was ineffective, giving no reaction after 12 h, also probably due to its low solubility. The experimental details of the oxidation of the parent C_6Ph_6 with $FeCl_3$ have not previously been reported to our best knowledge,[14] but this reagent has been used for substituted hexaphenylbenzenes. Because this oxidant is stronger and more soluble, the usual reaction time[17,61] is limited to 1 h. Analysis of the sample taken from the reaction mixture after 1 h confirmed the presence of the final product, HBC. Extending the reaction time to 12 h produced intractable material, which could not be characterized, even by MALDI- or LD-TOF mass spectroscopy. The mass balance of the $FeCl_3$ experiment exceeded 100%, suggesting that the product was contaminated by insoluble iron oxides.

Mechanistically relevant information was derived from gravimetric analyses of oxidations with substoichiometric oxidant. If partially oxidized intermediates (e.g., **15**, **167**) accumulate during the course of reaction, they will be present when a substoichiometric amount of oxidant is consumed.

For this reason, experiments with variable amounts of oxidants were performed. These experiments require quantitative mass balance data. Insoluble HBCwas isolated by filtration and exhaustive washing; purity was checked by MALDI-TOF MS and combustion analysis. Unreacted starting material C_6Ph_6 was isolated and its purity verified by HPLC with tandem UV−vis photodiode array (PDA) and evaporative light scattering (ELS) detectors and MALDI-TOF MS. Based on reported solubility of partially oxidized **14**, we anticipated that other partially oxidized intermediates would be soluble. In all cases, the yield of HBC and recovery of C_6Ph_6 accounted for all mass, within experimental uncertainty. In the case of oxidation by substoichiometric $CuCl_2$ (entries 9 and 10), we observed formation of a yet-unidentified soluble compound (~3%, ELS) the UV spectrum of which may correspond to a true intermediate. No other intermediates could be detected, and are therefore only present in trace (<1%) amounts.

Analysis of the insoluble crude HBC products from reactions using $MoCl_5$ by MALDI-TOF MS led to another interesting finding. Besides of major peak of HBC at $m/z = 522$, minor components corresponding to chlorinated derivatives of **10** ($m/z = 556$, 590, 624) could be detected. This finding was corroborated by combustion analysis of the crude reaction product, showing significant level of chlorination (C, 90.56; H, 4.38; Cl, 1.29).

SCHEME 13. Products from Oxidation of C_6Ph_6[a]

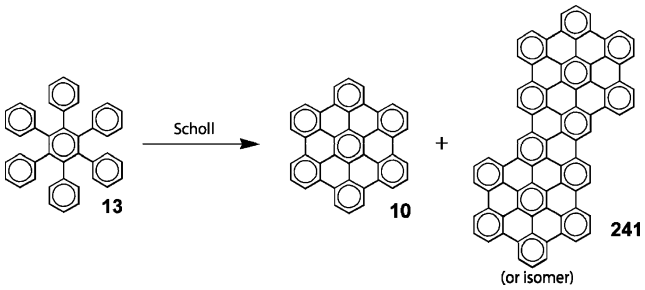

[a] Conditions: (a) $MoCl_5/CH_2Cl_2$, rt, 24 h; (b) $CuCl_2/AlCl_3/CS_2$, rt, 24 h; (c) $FeCl_3/CH_2Cl_2$, rt, 24 h; (d) $PhI(COCF_3)_2/BF_3{\cdot}Et_2O$, -40 °C, 3 h.

For all reaction conditions, intermolecular condensation products could be detected. For example, a peak at $m/z = 1038$, which corresponds to with condensed product **241** formed from two hexabenzocoronene units (Scheme 13), was observed. This dimer was observed in all samples, including those obtained using substoichiometric oxidant.

Concluding Remarks

The radical cation and arenium cation mechanisms of the Scholl reaction were investigated computationally. A comparison of these mechanisms, based on the thermodynamic assumption that the net energetic outcome is identical, reveals that the arenium cation mechanism involves lower energy transition states than the radical cation mechanism. In larger systems, the radical cation mechanism is more strongly disfavored. These findings are consistent with the literature reports of the Scholl reaction proceeding in acidic media that do not promote radical cation formation (anhydrous HF).[28] We believe that the Scholl reaction of unsubstituted oligophenylenes proceeds by an arenium cation mechanism, not a radical cation mechanism.

The thermodynamic calculations and kinetic analysis of the conversion of C_6Ph_6 to HBC suggest that intermediates will not accumulate in the course of the reaction. This contrasts with the results obtained by Halleux and by Müllen and co-workers. Halleux, however, did not report details of separation and characterization. Müllen and co-workers characterized the isolated intermediate—there is no doubt to its formation. This illustrates a shortcoming of our calculations—we are not modeling the actual system. The oxidant used, $CuCl_2$, is insoluble in carbon disulfide and the oxidation occurs on the $CuCl_2$ surface. The various intermediates certainly interact differently with the surface. In homogeneous reactions, we are unable to observe the accumulation of intermediates. We observe the formation of an HBC dimer or dimers, **241**, under all reaction conditions.

Several oxidation methods were tested and compared, which provided the opportunity for reaction optimization. The homogeneous oxidizing systems, $MoCl_5$ in CH_2Cl_2 and $PhI(O_2CCF_3)_2/BF_3{\cdot}Et_2O$ in CH_2Cl_2, were shown to be effective for the Scholl cyclization of C_6Ph_6 to HBC.

Experimental Section

General Methods. Reactants and reagents were used as received. CH_2Cl_2 was distilled from CaH_2 and stored over molecular sieves, and CS_2 was stored over $CaCl_2$. Good ventilation, protective

(63) Larson, M. L.; Moore, F. W. *Inorg. Chem.* **1964**, *3*, 285−286.

equipment, and absence of sources of ignition are vital for the safe handling of CS_2 due to its toxicity and low flash point.

Mass spectra were recorded on a MALDI-TOF MS instrument in reflector mode using an α-cyano-4-hydroxycinnamic acid matrix. HPLC analyses were done using a photodiode array detector and evaporative light scattering detector, employing a reversed-phase C_{18} column and a mobile-phase methanol−water (92:8).

General Procedure: Oxidation by $MoCl_5$, Cu(II) Salts, $FeCl_3$. To a solution of C_6Ph_6 (0.100 g, 0.187 mmol) in 10 mL of solvent was added an appropriate amount of oxidant (see Table 4), and the reaction mixture was stirred under nitrogen at rt for 12 h. Methanol (10 mL) was added and stirring continued for 1 h. The mixture was diluted with CH_2Cl_2 and methanol, and the insoluble HBC was collected by fitration. The solids were exhaustively washed with MeOH, CH_2Cl_2, MeOH, H_2O, MeOH, CH_2Cl_2, THF, benzene, and CH_2Cl_2. The filtrate was diluted with H_2O and extracted with CH_2Cl_2. The composition of the resulting CH_2Cl_2-soluble residue was analyzed by HPLC.

General Procedure: Oxidation by $PhI(O_2CCF_3)_2/BF_3{\cdot}Et_2O$. To a solution of 1,2,3,4,5,6-hexaphenylbenzene (0.100 g, 0.187 mmol) in CH_2Cl_2 (5 mL) was added dropwise an equimolar CH_2Cl_2 solution of $PhI(O_2CCF_3)_2$ and $BF_3{\cdot}Et_2O$ at −40 °C (see Table 4). The reaction mixture was stirred for 3.5 h while the temperature was allowed to rise to −10 °C. The reaction was quenched by MeOH and an aqueous solution of Na_2SO_3. The resulting mixture was worked up as described for $MoCl_5$ oxidations.

Acknowledgment. This work was supported by an award from the Research Corporation, the University of Nevada, the National Science Foundation (CHE-0449740), and the Office of Naval Research. Acknowledgment is made to the Donors of the American Chemical Society Petroleum Research Fund for partial support of this research.

Supporting Information Available: Optimized structures (Cartesian coordinates), energies, and thermodynamic arguments for the comparison of the arenium cation and radical cation mechanisms. This material is available free of charge via the Internet at http://pubs.acs.org.

JO0526744